CompressibilityAnalysis and Geomechanical Characterization for CO_2 Sequestration and Storage for Advancement of Health and Environment Protection. A Case of 'Jxt' Field, Niger Delta, Nigeria

ABSTRACT

CO_2 sequestration and storage are parts of the approaches to mitigate the effect of global warming through the reduction and stabilization of CO_2 emitted in the atmosphere. In the Niger Delta, several depleted and abandoned wells can be utilized as geologic storage for CO_2 to assist economic growth and environmental protection This study aimed at identifying suitable reservoirs for CO_2 storage to prevent it from leaking to the surface. Logs from two wells from the 'JXT' field, onshore, Niger Delta were used for the studies. Petrophysics computation and Rock physics analysis such as Geomechanics, fluid sensitivity and compressibility were carried out. Potential reservoirs were delineated and correlated, elastic parameters were generated from pseudo logs, cross plotted for comparison, and evaluated for physical strength. Fluid sensitivity was carried out using Gassmann's equation to understand dry rock sensitivity to fluid changes. Finally, a compressibility study was done to measure the drained and undrained properties of each reservoir and its resistance to compressive forces. Results of the petrophysical analysis for the three potential reservoirs (A, B, C) delineated revealed values ranging from a high thickness of reservoir (20-109m), moderate porosity (17-23%), and good permeability (128-1251mD). The geomechanical analysis for the two wells shows the range of values for Young modulus (E) as (20.5-27.5GPa), bulk modulus (k) as (21.3-25.3GPa), Shear modulus (μ) as (8.01-11.2GPa) and Poisson ratio (σ) as (0.25). Results from the compressibility analysis indicated the average drained and undrained compressibility for both wells as ($0.048GPa^{-1}$, $0.044GPa^{-1}$) and ($0.044GPa^{-1}$, $0.044GPa^{-1}$) respectively. Conclusively, the results indicated that the 'JXT' field is suitable for CO_2 storage and can be considered to reduce the emission of this greenhouse gas into the atmosphere and aid positive global climate change.

Keywords: Reservoir Characterization, CO_2 Sequestration, Rock Physics, Geomechanics, Petrophysics

INTRODUCTION

CO_2 and other greenhouse gases emitted daily into the Earth's atmosphere pose a great challenge to our existence as humans and the adverse effects in the form of climate change increasing every year [1,2, 3]. The environment is becoming almost inhabitable for us with the rise in average temperatures reaching critical points [1,4,5]. Melting glaciers are destroying natural habitats of endangered animals and causing a rise in sea levels. This in turn leads to flooding and poor quality of life. Flooding leads to the loss of lives and, the destruction of homes, farms, infrastructure, etc. [4,6,7] Cold regions of the world are becoming warmer, and warm regions are becoming hotter, natural habitats are gradually disappearing. The environment is the worst hit but we are the most affected [1,4,8] . The presence of these destructive substances is anthropogenic and can be attributed to human activities, and the desire to generate energy for self-sustainability and community development. [9,10]

Nigeria is the principal producer of oil and gas in Africa, and the Niger Delta basin is the predominant basin from which most of its crude oil is produced [11,12.13.14]. According to the World Development Indicator. Nigeria is ranked 39th in the world for CO_2 emissions from all sources, with emissions/discharges rising from 3,406.6kt in 1960 to 88,026kt in 2011, and contribute adding 0.3% of the worldwide/global emissions [15,16,17] In the exploration and production division or sector, Nigeria ranks in the top 1% for the emission of greenhouse gases in Africa, splaying 1.4 billion cubic feet of accompanying gas daily. This is equivalent to approximately 40% of the gas produced from over 120 flaring sites [16,18].

These events can hardly be reversed but can be mitigated, and the process slowed down. The Kyoto Protocol and the United Nations (UN) Context Convention on Climate Change were set up to achieve the objective of mitigating the effects of global warming and climate change by reducing the amount of CO_2 present in the atmosphere [4,6,19].

CO_2 capture and sequestration are processes that have been identified and adopted to mitigate and slow down the rate of CO_2 emission into the atmosphere [14,8,9]. It involves the capture of CO_2 before its emission into the atmosphere, and injection into deep subsurface formations for lengthy periods of storage and sequestration [1,7,20]]. The geologic sequestration of CO_2 into the subsurface, which includes depleted Oil and gas reservoirs, salt domes, and coal seam beds, requires initial characterization of the site where the CO_2 is to be sequestered, in terms of the geology, structural framework, and geomechanical properties [15]. This is done to determine the volume capacity of the reservoir, optimum conditions present for the long-term storage and containment of the CO_2, and the injectivity (permeability of the reservoir), for fluid flow [3,21,22].

Nigeria is a major player in the hydrocarbon exploration sector in Africa and globally, with several reservoirs explored, produced, depleted, and abandoned since the inception of the exploration industry of Nigeria in 1957 [12.23]. It is expected that these brownfields in the Niger Delta can be utilized for the geologic sequestration of CO_2[1012.14,24]. This will assist in better understanding of the physical properties of these reservoirs in terms of storage capacity, containment capacity, and injectivity, feasibility studies must be carried out [1,9, 10],

This work aims to study the compressibility and geomechanical properties of a reservoir using rock physics to analyze the suitability of the reservoir for CO_2 sequestration and storage in the future after the well has been depleted through production, and abandoned.

LOCATION AND GEOLOGY OF THE STUDY AREA

Situated in the Gulf of Guinea and extending throughout the Niger Delta domain, is the Niger Delta [11,12,25]. Delta prograde southwestward from the Eocene to the present, creating depo-belts that signify the most active percentage of the delta at each phase of its expansion [25,26]. These depo-belts become one of the major regressive deltas globally. One petroleum system identified in the Niger Delta province is the Tertiary Niger Delta. [12 13, 14, 27]. The main source rock remains in the upper Akata Formation, consisting of the marine-shale facies, probably influenced by interbedded marine shale in the lowermost Agbada Formation.[25,26,27]. Agbada Formation sandstone accommodates hydrocarbons, whereas the upper Agbada Formation turbidite sand units serve as potential reservoirs in deep water offshore [11, 12, 18, 23,]. Figure 1shows the location map of

the Niger Delta and the base map of the study area.
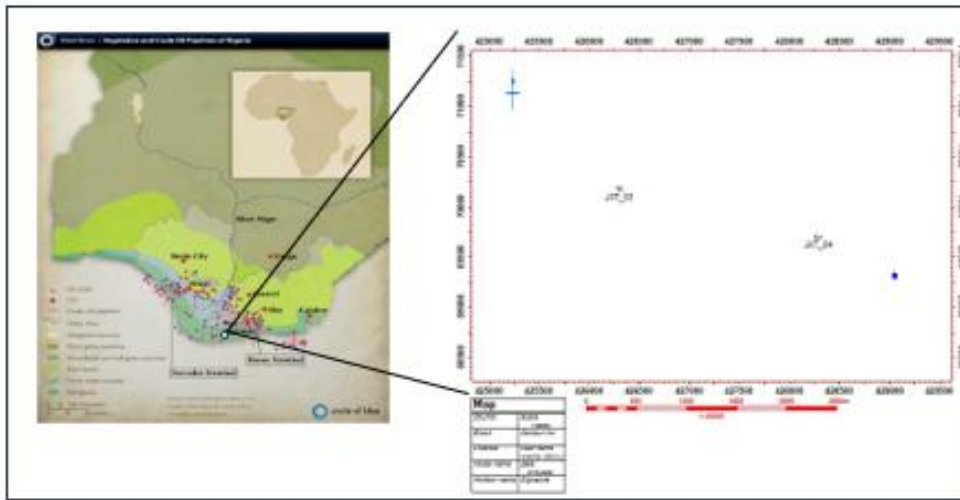
Figure 1: The location map of the Niger Delta and the base map of the study area.

METHODOLOGY

Two wells in the "JXT field", JXT_03 and JXT_04, equipped with suites of wireline logs, including lithology log (gamma ray), resistivity, and porosity logs (neutron, sonic, and bulk density), were utilized for this study. The methodology adopted for this study is grouped into two major sections. These include Petrophysical analysis and Rock physics analysis (Geomechanical and Compressibility analysis)

1. Petrophysical analysis

This section assists in conducting the compressibility analysis and elastic property characterization of the reservoir, as well as the sensitivity analysis of each elastic parameter utilized in this study [12]. The lateral variations and vertical thickness of delineated reservoir units were investigated by correlating the formation tops and lithology units across the field. Six petrophysical parameters were evaluated for the three delineated reservoir formations These include reservoir thickness, shale volume, porosity (effective), permeability, water saturation, and hydrocarbon saturation [11, 12, 13, 14,18, 28, 29].

Reservoir thickness

The gamma-ray log was handy in identifying the reservoirs in the 'JXT' field. The reservoir thickness (h) was calculated using the following relationship/ equations 1 to 7 [12,13,14]

$$h = Base\ Depth - Top\ Depth \quad (1)$$

Shale volume (V_{sh})

For the shale volume estimation, [14]. Larionov's (1969) equation for tertiary formations was used [23, 30].

$$Vsh = 0.083 (2^{3.7*Igr} - 1) \quad (2)$$

$$Igr = \frac{GR_{log} - GR_{min}}{GR_{max} - GR_{min}} \quad (3)$$

Where Igr is the gamma ray log index, GR_{log} is the gamma ray log appraisal at the depth of concentration, GR_{min} is the gamma ray log appraisal /reading in the clean zone, GR_{max} is the gamma ray log appraisal/reading in the shale zone. [12,13]

Porosity

Porosity aids estimation of compaction trends and differentiating the hydrocarbon zones using Neutron, and Density log [11,12,13,14].

$$\Phi = \sqrt{\frac{\Phi_{density}^2 + \Phi_{neutron}^2}{2}} \quad (4)$$

The effective porosity is given by Eq. 5 [19]

$$\Phi_{eff} = \Phi_{Total}(1 - V_{sh}) \quad (5)$$

Water saturation

Water saturation is obtained using the Archie. Equation. [7, 11],

$$Sw = \sqrt[n]{\frac{a * Rw}{\varphi^m * Rt}} \qquad (6)$$

Hydrocarbon saturation

For hydrocarbon saturation (S_h) was obtained using an equation defined by

$$S_h = (1 - Sw) \qquad (7)$$

2. Rock physics investigation

Rock physics analysis is used to establish the relationship between reservoir properties (porosity, volume of shale, and water saturation) and elastic properties (velocity, impedance, and density) [12, 30, 31, 32, 33]. Hence the primary focus of rock physics investigation is to meet the need to quantify and improve the interpretation of amplitudes for hydrocarbon discovery, reservoir characterization, and reservoir monitoring, especially with the recent improvements and developments in seismic data acquisition, and processing [12. 31, 34,]. Rock physics analysis is carried out to estimate the elastic properties/assets of the reservoir rocks identified in the 'JXT' field. The estimation of these elastic parameters aided the characterization of the reservoirs in terms of their lithology, fluid content, and Geomechanical properties (figure 2) [11,12,34]

Calculation of Rock Physics parameters

Equations 8 to 29 were used for the computation of the elastic parameters on the field. [12, 14,29, 31,
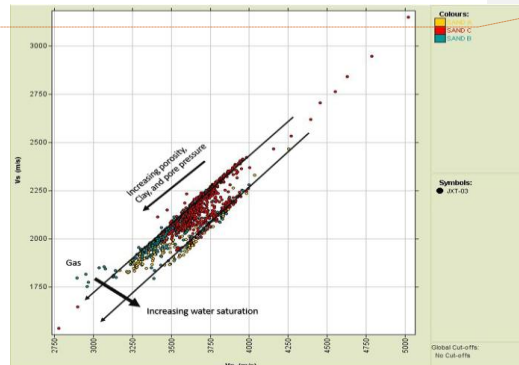
Vp estimation

Vp, known as compressional wave velocity, and the equation below was used to estimate Vp from the compressional wave sonic transit time log (DT$_c$).

$$Vp = \left(\frac{1000000}{DTc}\right) * 0.3281 \qquad (8)$$

Vs estimation

Shear wave velocity (Vs) is estimated from Vp using the following empirical relationships usingCastagna equation

$$Vs = 0.804Vp - 0.856 \qquad (9)$$

Figure 2: Cross-plot of Vs against Vp in JXT 03, digitized after [31].

Geomechanics

This deals with the behavior of rocks under the influence of different forces, with respect to their physical properties, and interaction under different stress regimes. Reservoir geomechanics is an area of rock mechanics that integrates the study of the stresses of the earth with the knowledge of the principles of rock mechanics across various disciplines to solve problems that may arise during the life cycle of 1`a reservoir, from exploration to abandonment 9, 14, 35].

Estimation of Geomechanical parameters

Bulk modulus (K)

The bulk modulus denotes the volumetric alteration/changes of a material under the influence of normal stresses [35, 36]. The dynamic bulk modulus of a reservoir formation describes the volume changes of the formation with respect to the fluid bulk modulus, under the influence of normal stresses. The equation below was used to derive the dynamic bulk modulus (K), in this study.

$$K = \rho * \left(Vp^2 - \frac{4}{3}Vs^2\right) \qquad (10)$$

Shear modulus (μ)

The shear of a formation describes the resistance of the formation to shearing stress (Telford *et al.* 1990).

$$\mu = \rho * (Vs)^2 \qquad (11)$$

Lambda (λ)

Lambda (λ) is among the class of elastic parameters known as Lame's parameters. In this study, it was used in the characterization of other Geomechanical parameters.

$$\lambda = \rho * (Vp^2 - \frac{2\mu}{\rho})$$ (12)

Young modulus (E)

Young modulus describes the longitudinal strains when uniaxial normal stress is applied to a material. In this study, E was derived using the relationship between Lambda (λ) and Mu (μ) [12, 14]

$$E = \mu * \left(\frac{3\lambda + 2\mu}{\lambda + \mu}\right)$$ (13)

Poisson ratio (σ)

The Poisson ratio measures the deformability of a rock formation and its ability to resist compressive forces. It is in the range of 0.05 to 0.5, with the former representing very hard materials, and the latter representing very soft materials.

$$\sigma = \frac{\lambda}{2(\lambda + \mu)}$$ (14)

Gassmann's model

Gassmann's model applied in this study is given in equation 15.

$$\frac{K_{sat}}{K_{mineral} - K_{sat}} = \frac{K_{dry}}{K_{dry} - K_{dry}} + \frac{K_{fluid}}{\phi(K_{min} - K_{fluid})}$$ (15)

$$\mu dry = \mu sat$$ (16)

where K_{sat} is the saturated bulk density, K_{dry} is the dry bulk density, K_{min} is the mineral bulk density, K_{fluid} is the fluid bulk density, μ_{dry} is the shear modulus of dry rock, μ_{sat} is the shear modulus of saturated rock, and ϕ is the effective porosity of the reservoir formation. [12,31]..

Compressibility analysis

The compressibility analysis describes the physical properties of the reservoir, in terms of its density. A rock with low porosity tends to have a high density, which translates to the bulk modulus of the rock frame. The compressibility is the inverse of the bulk modulus of the formation and is affected by the fluid contained in the pores of the formation [31, 33]. A weak formation with high porosity is expected to be highly compressible, while a stiff formation with low porosity is expected to be less compressible. [14].

The compressibility analysis carried out in this study was carried out in two phases, using the Gassmann equation, and the Berryman (1995) form of the Hashin-Shtrikman-Wadpole (1966) equation.

Gassmann's equation for compressibility analysis

The compressible form of equation 15 was adopted for the compressibility analysis carried out in this study [14,31]

$$(C_{sat} - C_{min})^{-1} = (C_{dry} - C_{min})^{-1} + [\emptyset(C_{fl} - C_{min})]^{-1}$$ (17)

$$C_{sat} = \frac{1}{K_{sat}}, \quad C_{dry} = \frac{1}{K_{dry}}, \quad C_{fl} = \frac{1}{K_{fl}}, C_{min} = \frac{1}{K_{min}}.$$ (18)

Where $\frac{1}{K_{dp}}$ is the dry pore compressibility, $\frac{1}{K_{sp}}$ is the saturated pore compressibility, and $\frac{1}{K_{\phi}}$ is the pore space compressibility.

Hashim-Shtrikman-Wadpole bounds for elastic moduli

According to Hashim-Shtrikman (1963), and Wadpole (1966) [14] ,the effective elastic moduli of a mixture of mineral grains and pores can be predicted (Figures 3 and 4). This can be achieved without specifying the geometric details of the phases' arrangements relative to each other [14,31]

$$K^{HS\pm} = K_1 + \frac{f_2}{(K_2 - K_1)^{-1} + f_1\left(K_1 + \frac{4}{3}\mu_m\right)^{-1}}$$ (19)

$$\mu^{HS\pm} = \mu_1 + \frac{f_2}{(\mu_2 - \mu_1)^{-1} + f_1[\mu_1 + \frac{\mu_m}{6}\left(\frac{9K_m + 8\mu_m}{K_m + 2\mu_m}\right)]^{-1}}$$ (20)
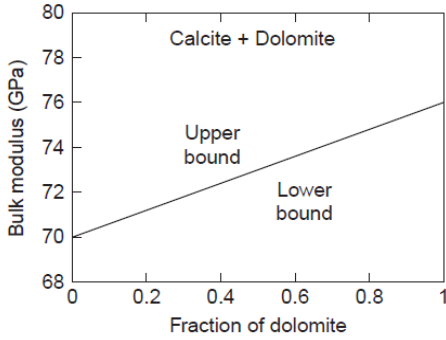
Figure 3: Plot of bulk modulus against volume fraction of mineral mixture in the Hashim-stickman bounds for elastic moduli (Avseth*et al.*, 2005).

greater The Berryman (1995) general method of the Hashim-Shtrikman-Wadpole model for a mixture than two phases were adopted to predict and envisage the effective elastic moduliof each reservoir identified in this study. [14]. The upper and lower bounds of the compressibility of each reservoir formation were estimated using this model.

$$K^{HS+} = \Lambda(\mu_{max}) \qquad (21)$$

$$K^{HS-} = \Lambda(\mu_{min}) \qquad (22)$$

$$\mu^{HS+} = \Gamma\big(\zeta(K_{max}, \mu_{max})\big) \qquad (23)$$

$$\mu^{HS-} = \Gamma\big(\zeta(K_{min}, \mu_{min})\big) \qquad (24)$$
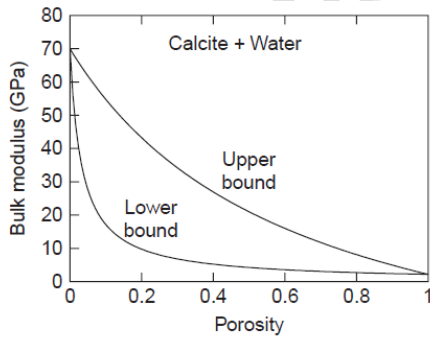
Figure 4: A plot of Bulk modulus against volume fraction of mineral and fluid mixture in the Hashim-shtrikman bounds for elastic moduli (Avseth*et al.*, 2005

Properties of the individual components (subscripts "1" and "2"). Equations (22) and

(23) produce the upper bound, maximum bulk, and shear moduli of the individual constituents and the lower bound are K_m and μ_m, while the minimum bulk and shear moduli of the constituents are K_m and μ_m. [37].

$$\Lambda(z) = \left\langle \frac{1}{K(r) + \frac{4}{3}z} \right\rangle^{-1} - \frac{4}{3}z$$

$$\Gamma(z) = \left\langle \frac{1}{\mu(r) + z} \right\rangle^{-1} - z$$

$$\zeta(K, \mu) = \frac{\mu}{6}\left(\frac{9K + 8\mu}{K + 2\mu}\right)$$

The brackets specify an average over the medium similar to an average over the constituents weighed using their volume fractions

Modified Hashim-Shtrikman-Wadpole bounds for compressibility analysis

To determine the upper bounds and lower bounds on the effective compressibility of a mixture of more than two phases, the Hashim-Shtrikman-Wadpole bounds model was adopted and modified in this study [14]. The upper bound of the effective compressibility is equivalent to the inverse of the lower bound on the effective elastic moduli of the mixture, while the lower bound of the effective compressibility is equivalent to the upper bound on the effective elastic moduli [14,31.38].

$$C^{HS+} = \frac{1}{K^{HS-}} \qquad (28)$$

$$C^{HS-} = \frac{1}{K^{HS+}} \qquad (29)$$

RESULTS AND DISCUSSION

Petrophysical analysis

The stratigraphy of the two wells in the JXT field shows an intercalation of shale and sandstone layers. Three reservoirs were delineated and correlated across the two wells, 'JXT' 03 and 'JXT' 04. The three reservoirs are SAND A, SAND B, and SAND C. The delineation and correlation of these lithologic units were achieved by using the gamma-ray and resistivity logs (Figure 5). The summary of the results from the petrophysical analysis carried out is shown in Tables 1 and 2.
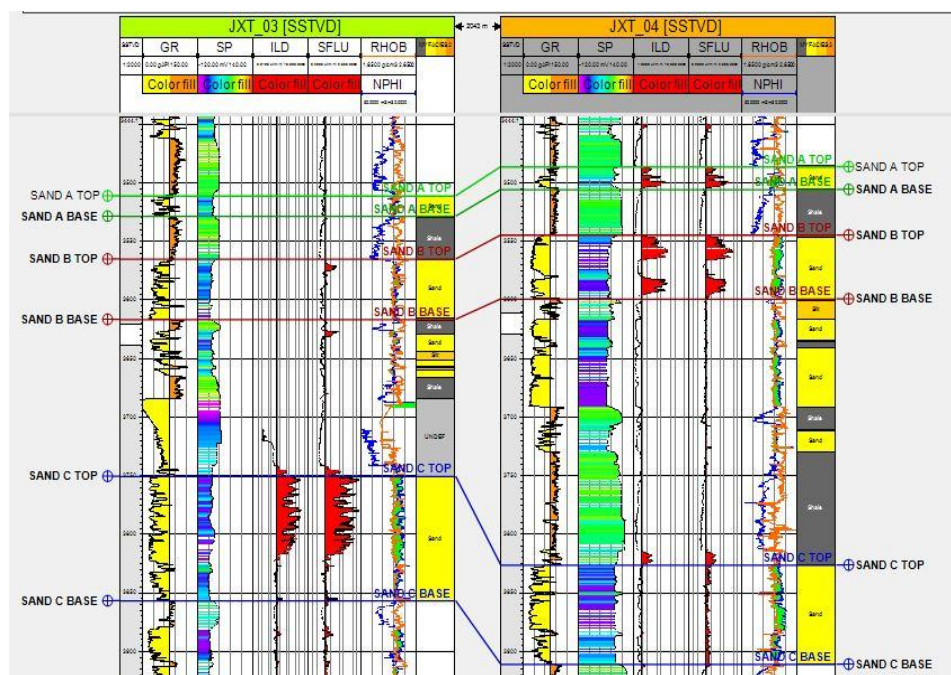
Figure 5: Reservoirs correlated across JXT 03 and 04.

Table 1**:** Summary of petrophysical evaluation of the reservoirs in JXT 03

PARAMETER	JXT-03		
Reservoirs	SAND A	SAND B	SAND C
MD (m) -Top	3510.13	3565.23	3750.25
-Base	3530.71	3618.28	3858.61
THICKNESS (m)	20.58	53.05	108.36
Vsh (%)	0.15	0.14	0.08
POROSITY (%)	0.2	0.2	0.23
PERMEABILITY (mD)	469.1	367	1251
Sw (%)	0.9	0.8	0.2
Sh (%)	0.1	0.2	0.8

Table 1: Summary of petrophysical evaluation of the reservoirs in JXT 04

PARAMETER	JXT-04		
Reservoirs	SAND A	SAND B	SAND C
MD (m) -Top	3485.27	3545.27	3827.63
Base	3505.69	3600.69	3910
THICKNESS (m)	20.42	55.42	82.37
Vsh (%)	0.21	0.12	0.12
POROSITY (%)	0.17	0.2	0.2
PERMEABILITY (mD)	128.1	310.2	310.2
Sw (%)	0.3	0.3	0.8
Sh (%)	0.7	0.7	0.2

SAND C ranges from a depth of 3750m to 3859m in JXT 03. The depth range of this reservoir gives it a thickness of about 108m. In JXT 04, this reservoir has an estimated thickness of about 82m and a depth range of 3828m to 3910m. The shale volume of SAND A has an estimated value of 8% in JXT 03 and 12% in JXT 04. Across the two wells, the effective porosity was estimated to be 23% and 20%respectively. The permeability of this reservoir ranges from 310mD in JXT 04 and 1251mD in JXT 03. The reservoir is highly saturated with hydrocarbons in JXT 03 at 80%, while in JXT 04, the water saturation increases to 80%. In this regard, the hydrocarbon saturation across both wells' ranges from 20% in JXT 04 to 80% in JXT 03.

Rock physics

The Vp across the SAND A interval in JXT 03 is 3489.1 m/s, while in JXT 04, it is 3402 m/s (Tables 3 and 4). In the SAND B interval, the Vp increases with values ranging from 3473 m/s to 3686.1 m/s. The lower Vp values for SAND A and B were estimated from JXT 04, while the higher values are from the JXT 03 well. The Vp values in the SAND C reservoir interval were estimated to have higher values in JXT 04, than in JXT 03. The increase and decrease in values of Vp across both wells can be attributed to changes in fluid saturation in the reservoirs. There is an observed increase when water saturation increases and a decrease when gas saturation increases.

The Vs across the reservoirs is unaffected by fluid because shear sonic waves do not travel through fluids [31]. The results from Vs estimation can be used to show the cementation properties in each of the reservoirs. The estimated Vs values from the SAND A interval across both wells range from 1887.5m/s to 1967m/s, with the higher values observed in JXT 03. The estimated values in SAND B show an increase in depth, and range from 2019.4m/s to 2170m/s, with the values increasing from JXT 03 to JXT 04. Vs values in SAND C range from 2214.4m/s to 2248m/s. The increase in Vs values across both wells indicates the direction of increasing cementation in the JXT field. For SAND A, cementation increases from SE to NW, while SAND B and C show an increase from the NW to SE direction. Cementation is important in understanding pore volume compressibility because it reduces the effect of compressive forces on the formation matrix. Studies have shown that formations with high cementation and low clay volume have higher effective porosities while undergoing diagenetic processes (Han, 1986; Avseth 2005).

Table 3: Calculated rock physics parameters of JXT 03

JXT 03				
	Vp	**Vs**	**Porosity**	**Rho**
SAND A	3489	1967	0.2	2.27
SAND B	3473	2019.4	0.2	2.26
SAND C	3746.2	2214.4	0.23	2.177

Table 4: Calculated rock physics parameters of JXT 04

JXT 04				
	Vp	**Vs**	**Porosity**	**Rho**
SAND A	3402.1	1887.5	0.17	2.25
SAND B	3686.1	2170	0.17	2.146
SAND C	3809.5	2248.3	0.19	2.209

Estimation of elastic parameters

The estimated bulk modulus of the reservoirs in the JXT field ranges from 21.3GPa to 25.3GPa, while the shear modulus ranges from 8GPa to 11.2GPa. Quartz being the major mineral in a clastic reservoir setting has a bulk modulus of 36.6GPa, therefore, the estimated bulk modulus of the reservoirs in the JXT field gives a good indication of its strength. The young modulus estimated also indicates the strength of the reservoirs. The values range from 20GPa to 28GPa, while the Poisson ratio ranges from 0.23 to 0.28. A detailed look at these results reveals that in terms of bulk modulus and young modulus, SAND A registered the lowest values across both wells, while SAND C registered the highest values. A summary of the estimated parameters is shown in Tables 5 and 6.

Table 5: A summary of the estimated reservoir elastic parameters in JXT 03

JXT 03				
	K(GPa)	**µ(GPa)**	**E(GPa)**	**Σ**
SAND A	22.5	8.8	22.3	0.27
SAND B	21.8	9.2	23	0.24
SAND C	24	10.67	26.3	0.23

Table 6: A summary of the estimated reservoir elastic parameters in JXT 03

JXT 04				
	K(GPa)	μ(GPa)	E(GPa)	Σ
SAND A	21.3	8	20.5	0.28
SAND B	22.9	10	25	0.23
SAND C	25.3	11.2	27.5	0.23

Compressibility Analysis

This involved using Gassmann's model and Modified Hashim-Shtrikman-Wadpole bounds for compressibility analysis

Gassmann's model

Gassmann's model estimation of saturated bulk modulus, mineral modulus, undrained pore modulus, drained pore modulus, fluid modulus, and dry rock modulus was implemented (Tables 6,7, 8, 9 and 10). This aided the estimation of the corresponding saturated rock compressibility, mineral compressibility, undrained pore compressibility, fluid compressibility, drained pore compressibility C(dp), and dry rock compressibility. From Tables 6 and 8, the drained pore compressibility C(dp), which is the pore volume compressibility of the reservoir formations ranges from $0.06GPa^{-1}$ to $0.13GPa^{-1}$. The values of the limits of compressibility derived from the Gassmann model were used to measure the pore volume compressibility relative to the mineral compressibility. Based on the obtained results, the SAND C reservoir has the least compressible pore volume. It is 2.2 times more compressible than quartz mineral. SAND A has the most compressible pore volume and is approximately 5 times more compressible than quartz mineral.

Table 7: Results for Ksat, Kmin, Ksp, Kdp, Kf, and Kdry, from the Gassmann compressibility analysis of JXT 03

		K(sat)	K(min)	K(sp)	K(dp)	K(f)	K(dry)	Por
	SAND A	22.5	36.6	11.7	8.91	2.77	20.1	0.2
WELL 3	SAND B	21.8	36.6	10.8	8	2.77	19.13	0.2
	SAND C	24.01	36.6	16.1	16	0.069	24	0.23

Table 8: Results for Csat, Cmin, Csp, Cdp, Cf, and Cdry, from the Gassmann compressibility analysis of JXT 03

		C(sat)	C(min)	C(sp)	C(f)	C(dp)	C(dry)
	SAND A	0.044	0.027	0.086	0.36	0.11	0.05
WELL 3	SAND B	0.046	0.027	0.093	0.36	0.13	0.052
	SAND C	0.042	0.027	0.062	14.5	0.063	0.042

Table 9: results for Ksat, Kmin, Ksp, Kdp, Kf, and Kdry, from the Gassmann compressibility analysis of JXT 04

		K(sat)	K(min)	K(sp)	K(dp)	K(f)	K(dry)	Por
	SAND A	21.3	36.6	8.7	0.17	0.069	21.23	
WELL 4	**SAND B**	22.9	36.6	11.6	11.6	0.069	22.85	0.19
	SAND C	25.3	36.6	15.6	12.8	2.77	23.72	0.19

Table 10: results for Csat, Cmin, Csp, Cdp, Cf, and Cdry, from the Gassmann compressibility analysis of JXT 04

		C(sat)	C(min)	C(sp)	C(f)	C(dp)	C(dry)
	SAND A	0.047	0.027	0.12	14.5	0.12	0.047
WELL 4	**SAND B**	0.044	0.027	0.086	14.5	0.087	0.044
	SAND C	0.04	0.027	0.064	0.36	0.08	0.042

Modified Hashim-Shtrikman-Wadpole bounds for compressibility analysis

The modified Hashim-shtrikman-wadpole model for compressibility is used in this research to predict the pore type within the allowable range [14. The pore types fall within the range of soft pore shapes and stiff pore shapes. Stiffer pore shapes made the compressibility values to be lower within the permissible range, while softer pore shapes caused the values to be higher. The results obtained from the application of this model are in the range of 0.04GPa^{-1} to 3GPa^{-1}. Where the lower bound of compressibility (C^{HS-}) measured in the JXT field is 0.04GPa^{-1}, while the upper bound of compressibility (C^{HS+}) is 3GPa^{-1}. In JXT 03, SAND A falls within the range of stiffer pore shapes (0.042GPa^{-1} to 0.38GPa^{-1}), SAND B falls within the range of stiffer pore shapes to moderately stiff pore shapes (0.042GPa^{-1} to 0.95GPa^{-1}), while SAND C falls within the range of softer pore shapes to stiffer pore shapes (0.042GPa^{-1} to 3GPa^{-1}). In JXT 04, SAND A falls within the range of stiffer to softer pore shapes (0.043GPa^{-1} to 2GPa^{-1}), SAND B falls within the range of stiffer to softer

pore shapes (0.04GPa^{-1} to 2.14GPa^{-1}), while SAND C falls within the region of stiffer pore shapes (0.04GPa^{-1} to 0.74GPa^{-1}) These values imply that the compressibility of a reservoir is highly influenced by lithology and mineral type, as well as fluid type. The results for each well are displayed in Tables 11 and 12.

Table 11: Results of the Hashin-Shtrikman-Wadpole compressibility analysis of JXT 03 highlighting the upper and lower boundaries.

WELL 3			
PARAMETER	**SAND A**	**SAND B**	**SAND C**
K(quartz)	36.6	36.6	36.6
K(shale)	11.4	11.4	11.4
K(gas)	0.069	0.069	0.069
K(water)	2.77	2.77	2.77
μ(quartz)	45	45	45
μ(shale)	3	3	3
μ(gas)	0	0	0
μ(water	0	0	0
K(SH+)	23.9	23.9	23.3
K(SH-)	2.605	1.054	0.34
C(SH+)	0.38	0.95	2.97
C(SH-)	0.042	0.042	0.043
μ(SH+)	23.4	23.8	24.6
μ(SH-)	0	0	0
Por	0.2	0.2	0.23
(1-Por)	0.8	0.2	0.8
Vquartz	0.85	0.86	0.92
Vsh	0.15	0.14	0.08
Sw	0.9	0.7	0.2
Sg	0.1	0.3	0.8

ζ(Kmax,μmax)	40.8	40.8	40.8

Table 12: Results of the Hashin-Shtrikman-Wadpole compressibility analysis of JXT 04 highlighting the upper and lower boundaries.

WELL 4			
PARAMETER	SAND A	SAND B	SAND C
K(quartz)	36.6	36.6	36.6
K(shale)	11.4	11.4	11.4
K(gas)	0.069	0.069	0.069
K(water)	2.77	2.77	2.77
μ(quartz)	45	45	45
μ(shale)	3	3	3
μ(gas)	0	0	0
μ (water)	0	0	0
K(SH+)	23	24	24.8
K(SH-)	0.5	0.47	1.35
C(SH+)	2.0	2.14	0.74
C(SH-)	0.043	0.04	0.04
μ(SH+)	22.5	25	25.
μ(SH-)	0	0	0
Por	0.17	0.19	0.19
(1-Por)	0.83	0.81	0.81
Vquartz	0.79	0.88	0.88
Vsh	0.21	0.12	0.12
Sw	0.3	0.3	0.8

Sg	0.7	0.7	0.2
ζ (Kmax, μmax)	40.84	40.84	40.84

CONCLUSION

There is a crucial need to mitigate the adverse effects of CO_2 emissions in the atmosphere which cause global warming,impacting both health and the environment negatively. This can be done through possible reduction and stabilization of CO_2 emitted in the atmosphere. In this study, CompressibilityAnalysis and Geomechanical Characterization were carried out for potential CO_2 Sequestration and Storage. This, in turn, will provide positive indications for the advancement of health and environmental protection. This study facilitated in the identification of the availability of suitable reservoirs for CO_2 storage to prevent this gas leakage to the surface. Logs from two wells from the 'JXT' field, onshore, Niger Delta were used for the study. Due to many years of hydrocarbon production in the Niger Delta, several depleted and abandoned wells that can be utilized as geologic storage for CO_2,supporting economic growth and environmental protection, are available. Results from Petrophysics and Rock physics (Geomechanics, fluid sensitivity, compressibility) analysis for comparison and evaluation of physical strength, rock sensitivity to fluid changes, the drained and undrained properties of each reservoir, and its resistance to compressive forces indicated that the 'JXT' field is suitable for CO_2 storage. It can therefore be considered for safe storage of CO_2 to reduce the emission of this greenhouse gas into the atmosphere. The study has shown that the availability of adequate, non-leaking reservoirs in the field can assist in health and environmental protection as it will aid positive global climate change.

COMPETING INTERESTS
Authors have declared that no competing interests exist.

REFERENCES

1. Yao J, Han H, Yang Y, Song Y, Li G. A Review of Recent Progress of Carbon Capture, Utilization, and Storage (CCUS) in China. *Applied Sciences.* 2023; 13(2):1169. https://doi.org/10.3390/app13021169

2. Chen et al. A critical review on deployment planning and risk analysis of carbon capture, utilization, and storage (CCUS) toward carbon neutrality. 2022, https://doi.org/10.1016/j.rser.2022.112537

3. Chen, Q.; Gu, Y.; Tang, Z.; Sun, Y. A carbon emission reduction scheme centered on the large-scale utilization of carbon dioxide. *Proc. Chin. Acad. 0Sci.* **2019**, *34*, 478–487.

4. Mikhaylov, A.; Moiseev, N.; Aleshin, K.; Burkhardt, T. Global climate change and greenhouse effect. *Entrep. Sustain. Issues* **2020**, *7*, 2897.

5. Chen, W. Building a carbon cycle model and improving the carbon emission reduction capacity-Sinopec started building China's first million-ton CCUS project. *Environ. Econ.* **2021**, *13*, 58–59.

6. Hegerl, G.C.; Ulrich, C. Greenhouse gas induced climate change. *Environ. Sci. Pollut. Res.* **1996**, *3*, 99–10.

7. Li, L.; Zhao, N.; Wei, W.; Sun, Y. A review of research progress on CO_2 capture, storage, and utilization in Chinese Academy of Sciences. *Fuel* **2013**, *108*, 112–130.

8. Cai, B.; Li, Q.; Zhang, X. *2021 Annual Report on CO_2 Capture Utilization and Storage in China: China's CCUS Pathways*; Ministry of Ecology and Environment of China: Beijing, China, 2021.

9. Yuan, S.; Ma, D.; Li, J.; Zhou, T.; Ji, Z.; Qi, X.; Han, H. Progress and prospects of carbon dioxide capture, EOR-utilization and storage industrialization. *Pet. Explor. Dev.* **2022**, *49*, 1–7G

Comment [DSS5]: This is not conclusion.

Comment [DSS6]: Modification needed.

10. Hannis, S.; Lu, J.; Chadwick, A.; Hovorka, S.; Kirk, K.; Romanak, K.; Pearc, J. CO_2 storage in depleted or depleting oil and gas fields: What can we learn from existing projects? *Energy Procedia* **2017**, *114*, 5680–5690.

11. Abe James Sunday Abe, Edigbue Paul Irikefe, Lawrence SamuelGbolahan."Rock physics analysis and Gassmann's fluid substitution for reservoir characterization of "G" field, Niger Delta", Arabian Journal of Geosciences. 2018, 11(21) DOI-10.1007/s12517-018-4023

12. Ojo B.T, Olowokere, M.T, Oladapo M.I. Sensitivity analysis of changing Reservoir Saturation involving Petrophysics and Rock Physics in 'Royal G' field, Niger Delta, *Results in Geophysical Sciences*, 2021,1(7). https://doi.org/10.1016/j.ringps.2021.100 018.).

13. Okpoli, C. C. Arogunyo. D. I "Integration of Well Logs and Seismic Attribute Analysis in Reservoir Identification on PGS Field Onshore Niger Delta, Nigeria", Pakistan Journal of Geology, 2020, 4(1) 12-22. DOI- 10.2478/pjg-2020-0002.

14. IdowuChukwudi, OjoB.T. Application of Gassmann's Model and the Modified Hashim-Shtrikman-Walpole Model in Land Subsidence Susceptibility Studies in the 'Jxt' Field, Niger Delta. One petro, Society of Petroleum Engineers. 2022. 1-15,https://doi.org/10.2118/211960-MS.

15. Baines, S.J.; Worden, R.H. Geological storage of carbon dioxide. *Geol. Soc. Lond. Spec. Publ.* **2004**, *233*, 1–6G

16. World Bank: Identification for Development. 2015 (https://doi.org/10.1596%2F26437)

17. World Bank Book :Co_2 Emissions from Fuel Combustion (OECD), 2011 {https://doi.org/10.1787%2Fco2_fuel-2011-en}

18. Maju-Oyovwikowhe G. E., Lucas. F. A. :"Sedimentological Analysis of Core Samples to Decipher Depositional Environments: A Case Study of 'Valz-01' Well Niger-Delta Basin, Nigeria", Current Journal of Applied Science and Technology. 2019 Pp1-16, http://dx.doi.org/10.9734/cjast/2019/v36i 330237

19. Wilkes, M.D.; Mukherjee, S.; Brown, S. Linking CO_2 capture and pipeline transportation: Sensitivity analysis and dynamic study of the compression train. *Int. J. Greenh. Gas Control* **2021**, *111*, 103449.

20. Zhou, J. Feasibility analysis of CO_2-enhanced shale gas exploitation and geological storage. In Proceedings of the National Symposium on Special Gas Reservoir Development Technology, Beijing, China, 26–28 March 2013.

21. Alper, E.; Orhan, O.Y. CO_2 utilization: Developments in conversion processes. *Petroleum* **2017**, *3*, 109–126.

22. Buss, W.; Jansson, S.; Wurzer, C.; Mašek, O. Synergies between BECCS and biochar—Maximizing carbon sequestration potential by recycling wood ash. *ACS Sustain. Chem. Eng.* **2019**, *7*, 4204–4209

23. Ojo, B.T., Olowokere, M.T., and Oladapo, M.I, (2018). Quantitative Modeling of the Architecture and Connectivity Properties of Reservoirs in 'Royal' Field, Niger-Delta. Journal of Applied Geology and Geophysics, IOSR Journal 2018, 6(2) 1-*10*. DOI:10.9790/0990-0602020110.

24. Zhang, Z.; Zhou, M.; Sun, J.; Fang, C. Discussion on the utilization of carbon dioxide carboxylation. *Prog. Chem. Ind.* **2019**, *38*, 229–243

25. Doust, H., Omatsola, E.,. Niger delta. In: Edwards, J.D., Santogrossi, P.A. (Eds.), Divergent/passive Margin Basins. AAPG, Tulsa,1989. pp. 239e248.

26. Hospers, J., 1965. Gravity field and structure of the Niger delta, Nigeria, West Africa. Geol. Soc. Am. Bull. 76, 407e422.

27. Kulke, H.,. Nigeria. In: Kulke, H. (Ed.), Regional Petroleum Geology of the World. Part II: Africa, America, Australia and Antarctica. GebrüderBorntraeger, Berlin, 1995, pp. 143e172.

28. Lyaka, Aneth L., Mulibo, Gabriel D.: "PetrophysicalAnaly of the Mpapai well Logs in the East Pande Exploration Block, Southern Coast of Tanzania: Geological Implication on the Hydrocarbon Potential", Open Journal of Geology. 2018, 8(8), 781-802. DOI-10.4236/ojg.2018.88046.

29. Pervez Khalid. 'Effect of reservoir heterogeneities on elastic and seismic properties of Lower Cretaceous Sand Intervals, Lower Indus Basin of Pakistan", ActaGeodynamica et Geomaterialia, 2011, 2021. PP451-459. {https://doi.org/10.13168%2Fagg.2021.0032

30. Bosch Miguel, MukerjiTapan, Gonzalez EzequielF..: Seismic, rock physics, spatial models, and their integration in reservoir geophysics", Society of Exploration Geophysicists.2014, http://dx.doi.org/10.1190/1.978156080303027.entry7

31. Per Avseth, TapanMukerji, Gary Mavko. "Introduction to rock physics", Cambridge University Press (CUP). 2005, 359 pages10.

32. Saenger Erik H., Krüger, Oliver S., Shapiro, Serge A: "Effective elastic properties of fractured rocks: Dynamic vs. static considerations", SEG Technical Program Expanded Abstracts. 2006, http://dx.doi.org/10.1190/1.2369912

33. Gary Mavko, TapanMukerji, Jack Dvorkin.: "Effective Elastic Media: Bounds and Mixing Laws", Cambridge University Press (CUP). 2020, 220-308 http://dx.doi.org/10.1017/9781108333016.005

34. Ritesh Kumar Sharma, Satinder Chopra, Larry Lines."Seismic reservoir characterization of the Bone Spring and Wolf camp Formations in the Delaware Basin: Challenges and uncertainty in characterization using rock physics — A case study: Part 2", Interpretation. 2020, 8(4). T1057--T1069

35. Ruiz, Franklin J.; "Porous grain model and equivalent elastic medium approach for predicting effective elastic properties of sedimentary rocks", Proquest,2011, 20111003

36. SrinivasanGopalakrishnan: Wave Propagation in Viscoelastic Waveguides, {Elastic Wave Propagation in Structures and Materials} 2022, 129-156 {https://doi.org/10.1201%2F9781003120568-5

37. Afif, Omar Hussein Omar: "Rock Physics Modeling for a Clastic Reservoir in Saudi Arabia.", King Fahd University of Petroleum and Minerals (Saudi Arabia).2020.

38. Schreyer, Howard L., Lampe, Brandon C, Schreyer, Lynn G., Stormont, John C.Microscale analysis demonstrating the significance of shear and porosity in hydrostatic compression of porous media", International Journal of Rock Mechanics and Mining Sciences. 2021. Vol145. http://dx.doi.org/10.1016/j.ijrmms.2021.104751

[1]